



Acetic acid-leachable elements in pedogenic carbonate nodules and links to the East-Asian summer monsoon



Shiling Yang*, Zhongli Ding, Zhaoyan Gu

Key Laboratory of Cenozoic Geology and Environment, Institute of Geology and Geophysics, Chinese Academy of Sciences, Beijing 100029, China

ARTICLE INFO

Keywords:

Loess
Paleosol
Carbonate nodule
Elemental composition
Mineralogical composition
East-Asian summer monsoon

ABSTRACT

Carbonate nodules at the base of paleosols within Chinese loess are products of pedogenic neof ormation and thus have great potential to document the summer monsoon history. Here we present mineralogical and elemental compositions of carbonate nodules from a north–south loess transect of northern China for the last and penultimate interglacials. X-ray diffraction patterns show that the nodules are composed mainly of calcite, together with some silicate minerals such as quartz, plagioclase, orthoclase, illite, and kaolinite. Elemental composition of the acetic acid-leachable fraction is characterized by extremely high Ca concentration and modest K and Mg content, followed by Al, Si, Sr, Mn, Fe, P, Na, Ba, Pb, Th, and U. Based on the mineralogical data and relationship between carbonate and the leachable element content, we suggest that K, Mg, Sr, Ba, and U mainly come from clay minerals, Na from highly soluble salts trapped by calcite particles, and Al and Si from amorphous phases of pedogenic origin. For both the last and penultimate interglacials, the Na content decreases from north to south, while the Al, Si, and U concentrations show a southward-increasing pattern. These characteristics all suggest a southward decrease in aridity across the Chinese Loess Plateau for both interglacials, consistent with the pattern of a southerly increase in pedogenic development for the two interglacial soils, and with the pattern of the present north–south rainfall gradient. Therefore, Na/Al and Na/Si ratios in the acetic acid extract are efficient proxies for aridity and are ultimately controlled by the summer monsoon precipitation, i.e. high ratios indicate weakened summer monsoon intensity. In addition, the significant content of highly soluble Na salts in carbonate nodules highlights soil dewatering as an important mechanism for the formation of pedogenic carbonate, at least in the case of the northern Loess Plateau.

© 2013 Elsevier B.V. All rights reserved.

1. Introduction

Chinese loess deposits, with an area of 440,000 km², were transported by the East-Asian winter monsoon from the arid regions in northwestern China (An et al., 1991a; Liu, 1985; Liu and Ding, 1998; Yang and Ding, 2008). On the Chinese Loess Plateau, complete loess sequences consist of over 30 loess–soil couplets, which date back to ~2.8 Ma (Ding et al., 1993; Rutter et al., 1991; Xiong et al., 2003; Yang and Ding, 2010). The yellowish loess beds were deposited during cold, dry glacial periods, whereas the brownish or reddish soils developed in warm, humid interglacials (Ding et al., 1993; Kukla, 1987; Liu, 1985). From glacial to interglacials, the East-Asian winter monsoon weakened, while the summer monsoon strengthened (An et al., 1991b; Liu and Ding, 1998; Rutter and Ding, 1993; Yang and Ding, 2008). Thus the alternation of loess and soils documents large-amplitude oscillations of the winter and summer monsoons on orbital timescales.

The East-Asian summer monsoon is the main moisture carrier for the Loess Plateau, with over 70% of annual rainfall occurring in summer.

Therefore, chemical weathering intensity of loess deposits is widely used as a proxy for the East-Asian summer monsoon variations, and it is mostly quantified by a suite of elemental ratios such as Ba/Sr (Ding et al., 2001a; Gallet et al., 1996), Th/U (Gallet et al., 1996; Gu et al., 1997), Rb/Sr (Chen et al., 1999), Na/Al (Gu et al., 1999), Chemical Index of Alteration (CIA) (Liu et al., 1995; Xiong et al., 2010), Fe₂O₃(free)/Fe₂O₃(total) (Ding et al., 2001b; Guo et al., 2000), and (CaO + Na₂O + MgO)/TiO₂ (Yang et al., 2006). However, chemical weathering intensity reflected by most of these proxies is a combined result of chemical weathering in dust sources and sinks, and that caused by transport-induced particle size differentiation (Eden et al., 1994; Gu et al., 1997, 1999; Yang and Ding, 2004; Yang et al., 2006). It is only the signature resulting from post-depositional weathering that can be linked to summer monsoon intensity. In this regard, authigenic clay and carbonate minerals, products of soil-forming processes, are ideal materials for the reconstruction of summer monsoon. However, many of the clay minerals in loess and paleosol units are mainly detrital, rather than pedogenic origin (Ji et al., 1999; Liu, 1985), as the Chinese loess–paleosol deposits have experienced only the incipient and early stages of chemical weathering (Chen et al., 1998; Han et al., 1998). This makes it difficult to distinguish and separate authigenic from detrital clay minerals.

* Corresponding author. Tel.: +86 10 82998526; fax: +86 10 62010846.
E-mail address: yangsl@mail.iggcas.ac.cn (S. Yang).

During pedogenic processes, Ca^{2+} , released during dissolution of Ca-bearing minerals (mainly detrital calcite), are transported downward by precipitation-recharged soil water, and eventually reprecipitate as pedogenic carbonate at depth. Thus elemental and isotopic compositions of pedogenic carbonate have great potential to document local climate conditions. Carbonate nodules, a common form of pedogenic carbonate, are abundant at the base of most interglacial paleosols. To date, numerous isotopic studies of carbonate nodules from Chinese loess have been performed to investigate the history of vegetation and paleomonsoon (Ding and Yang, 2000; Han et al., 1997; Jiang et al., 1995, 1998; Wang and Zheng, 1989; Yang et al., 2012). However, little is known about the elemental composition of the carbonate nodules. On the Loess Plateau, there is a pronounced north–south climatic gradient in both present and past interglacials (Derbyshire et al., 1995; Yang and Ding, 2003; Yang et al., 2012). This provides a unique opportunity to evaluate the relationship between elemental composition of carbonate nodules and the summer monsoon.

This study presents the carbonate content, mineral and elemental compositions of carbonate nodules from a north–south loess transect for the last and penultimate interglacials. The aim is to identify the spatial pattern of elemental composition of carbonate nodules and to address its paleoclimatic implications.

2. Setting and stratigraphy

Our study transect runs north–south from Hongde near the Mu Us desert margin, to Yangling in the southernmost part of the Loess Plateau (Fig. 1). Four loess sections located at Hongde, Baimapu, Binxianbei, and Yangling were studied (Fig. 1). At present, the mean annual temperature and precipitation are 8.2 °C and 380 mm at Hongde, 8.5 °C and 500 mm at Baimapu, 10 °C and 560 mm at Binxianbei, and 13 °C and 630 mm at Yangling. Both mean annual temperature and rainfall increase southward along the loess transect (Fig. 1).

All loess sections consist of the loess(L)–soil(S) sequence S0, L1, S1, L2, and S2 (Fig. 2). The Holocene soil, S0, is characterized by a massive structure, relatively abundant dark organic matter and a few white-colored secondary carbonate pseudomycelia. The loess units L1 and L2

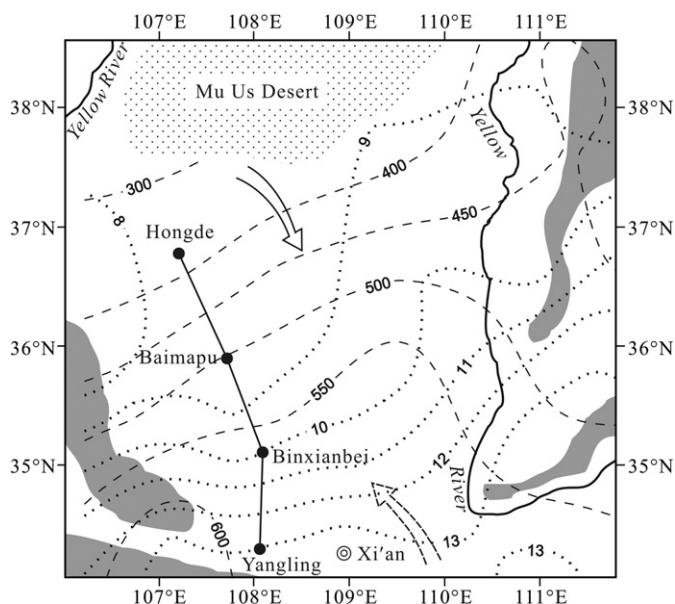


Fig. 1. Schematic map showing the location of the sites along the north–south transect on the Loess Plateau. Also shown are the Mu Us desert (dotted) and mountains (shaded) around and within the Plateau. The isohyets (mm, dashed lines) and isotherms (°C, dotted lines) are averaged values over 32 years (1970–2001). The solid and dashed arrows indicate the direction of the winter and summer monsoonal winds, respectively.

were deposited during the last and penultimate glacial periods, respectively. Both L1 and L2 are yellowish in color and massive in structure. Previous studies (Ding et al., 2002; Kukla, 1987; Lu et al., 2007) have shown that L1 is correlated with marine oxygen isotope stages (MIS) 2 to 4, and the L2 loess unit with MIS 6. The soil units S1 and S2 developed in the last and penultimate interglacial periods and correlate with MIS 5 and 7, respectively (Ding et al., 2002; Kukla, 1987; Lu et al., 2007). Both are brownish or reddish in color, and have an A-Bw-Bk-C or A-Bt-Bk-C horizon sequence. Soil unit S2 is composed of two soils (S2-1 and S2-2) and a thin intervening loess horizon. Only the upper soil (S2-1) was sampled in this study, as it is better developed than the lower one (S2-2). From Hongde southward to Yangling, the thickness of the loess units L1 and L2 decreases from over 20 m to several meters, while that of the soil units S1 and S2-1 decreases from 3–5 m to ~1.5 m. Based on a stacked orbital timescale of Chinese loess (Ding et al., 2002; Fig. 2), the soil units S1 and S2-1 formed in the periods 128–73 ka and 219–190 ka, respectively.

Carbonate nodules, with grayish color and sub-spherical or irregular shape, are commonly found at the base of paleosols but are rare within loess units. Generally, nodules at the base of the Holocene soil (S0) are sporadic and small (<1.5 cm) and can be found only in the central and southern Loess Plateau. For the soil units S1 and S2-1, nodule sizes range from a few centimeters in the north to over 10 cm in the south. At each transect site, carbonate nodules were taken from the base of soil units S1 and S2-1.

3. Materials and methods

For all the sections, a total of 2512 samples were collected at 5 cm intervals. Bulk magnetic susceptibility and grain size were measured for all samples with a Bartington MS2 susceptibility meter and a SALD-3001 laser diffraction particle analyser. The particle analytical procedures were detailed by Ding et al. (1999). Eight carbonate nodules (~2 g) taken from the base of S1 and S2-1 were ground to powder and split into three parts for analyses of carbonate content and mineralogical and elemental compositions. Carbonate content was determined using the gravimetric method (Soil Conservation Service, 1972) and has an error of $\pm 5\%$. The mineralogical composition was determined by X-ray diffraction (XRD) using a PANalytical X'Pert PRO diffractometer with a Ni-filtered $\text{CuK}\alpha$ radiation (40 kV, 40 mA). A 0.0625° divergence slit and a 0.125° anticatter slit were used. Powder samples, smeared on a glass slide with distilled water, were scanned from 2.5° to $70^\circ 2\theta$ with a step size of $0.0167^\circ 2\theta$ and a measuring time of 0.3 s per step.

Elemental composition of samples was analyzed by inductively coupled plasma mass spectrometry (ICP-MS) at the University of Arizona. Ground samples (~0.1 g) were first treated with 0.2 M NH_4 -acetate with a pH 8.2 for 4 h to minimize the effects of adsorbed cations, and then digested for at least 12 h in 0.2 M ultrapure acetic acid at room temperature to dissolve the carbonate fraction. After dissolution, carbonate digest was centrifuged, decanted, and rinsed with 18 M Ω H_2O . The supernatant was then dried down on a hotplate, redissolved in 1.5% ultrapure HNO_3 , and analyzed using a PerkinElmer Elan DRC II ICP-MS. Analytical uncertainties are $\pm 5\%$ for Ca content, and $\pm 10\%$ for content of other elements. This acetic acid leaching method has been widely used to measure the elemental and isotopic compositions of carbonate fraction in carbonate/silicate mixtures such as pedogenic carbonate (Quade et al., 1995; Van der Hoven and Quade, 2002), carbonate rocks (English et al., 2000), and ocean sediments (Lyle et al., 1984), and the acetic acid-leachable elements have been used to reconstruct paleoenvironmental conditions.

4. Results

4.1. Magnetic susceptibility and grain size

Paleosols are characterized consistently by higher susceptibility values and finer particle sizes compared with the loess horizons above

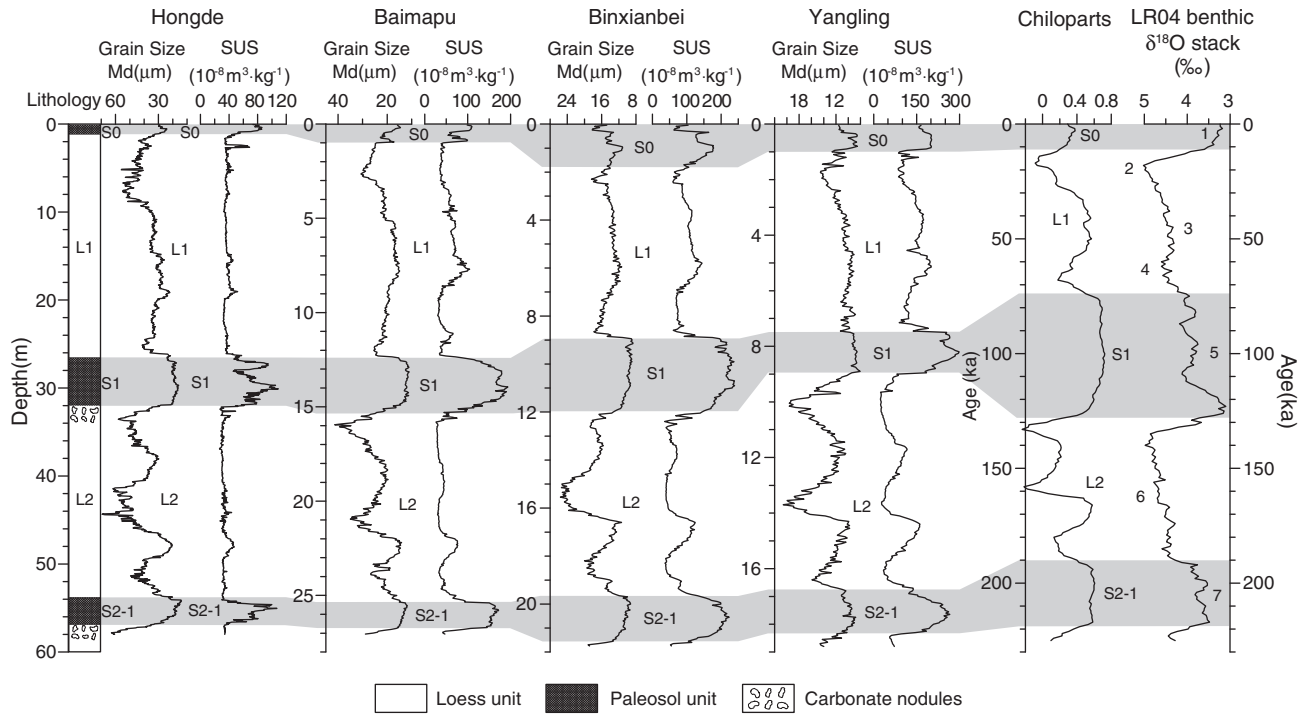


Fig. 2. Stratigraphic column, median grain size (Md), and magnetic susceptibility (SUS) for the Hongde–Yangling loess transect, and correlation with a stacked Chinese loess particle size record (Chiloparts) (Ding et al., 2002) and a stacked benthic $\delta^{18}\text{O}$ record (Lisiecki and Raymo, 2005). Marine isotope stages 1–7 are labeled. The shaded zones indicate interglacials.

and below them (Fig. 2). From Hongde southward to Yangling, the median grain size decreases from 50–60 μm to 15–20 μm for the typical loess units within L1 and L2, with the increase in magnetic susceptibility from 30–40 $\times 10^{-8} \text{ m}^3 \cdot \text{kg}^{-1}$ to 30–100 $\times 10^{-8} \text{ m}^3 \cdot \text{kg}^{-1}$. For the soil units S1 and S2-1, the median grain size decreases from 15–20 μm to 8–10 μm along the north–south transect, and the magnetic susceptibility increases from 80–110 $\times 10^{-8} \text{ m}^3 \cdot \text{kg}^{-1}$ to 240–300 $\times 10^{-8} \text{ m}^3 \cdot \text{kg}^{-1}$. These spatial patterns of grain size and magnetic susceptibility coincide with the pattern of a southerly increase in pedogenic development for both loess and soil units (Derbyshire et al., 1995; Huang et al., 2012; Yang and Ding, 2003), and with the pattern of the present north–south climatic gradient (Fig. 1).

4.2. Mineralogical composition

Carbonate content of the nodules ranges from 50 wt.% to 68 wt.% (Table 1). Thin sections show a brown micritic ground mass for all the carbonate nodules, throughout which are dispersed detrital grains mainly of quartz and feldspar. These detrital grains, coarse silt in size, comprise ~20–30% of the nodule volume. XRD shows a similar mineralogical composition for all the carbonate nodule samples (Fig. 3),

characterized mainly by calcite together with some silicate minerals such as quartz, plagioclase, orthoclase, and illite. Kaolinite is identified in all the nodule samples except those from the base of the soil unit S1 at Binxianbei and Yangling, while the peak of chlorite is recognized only in the nodule of S2-1 at Yangling. The clay mineral composition of carbonate nodules is consistent with that of Chinese loess (Gylesjö and Arnold, 2006).

4.3. Elemental composition

Elemental composition of the acid-leachable fraction of the carbonate nodules is shown in Table 1. Ca is unsurprisingly the most abundant element (range 190,000–250,000 ppm), followed by K (2000–8500 ppm) and Mg (1500–3300 ppm). Some elements are present in significant abundances, such as Al (~100–250 ppm), Si (~40–200 ppm), Sr (50–150 ppm), Mn (20–80 ppm), Fe (up to ~80 ppm), P (up to ~70 ppm), Na (15–40 ppm), and Ba (~10–20 ppm), while other detectable elements (e.g., Pb, Th, and U) are present in lower concentrations (mostly <1 ppm).

Spatial changes in concentration of some selected elements are shown in Fig. 4. From north to south, the Na content decreases gradually

Table 1

Carbonate contents (wt.%) and elemental concentrations (ppm) of the acetic acid-leachable fraction for carbonate nodules from soil units S1 and S2-1.

Sample	Carbonate (wt.%)	Na	Mg	Al	Si	P	K	Ca	Fe	Mn	Sr	Ba	Pb	Th	U
Hongde S1	54.3	36.8	2237	96	40	56.8	3772	195,221	5.3	53.3	99	22.5	0.57	0.46	0.31
Baimapu S1	63.2	37.8	1835	156	130	30.7	4221	236,730	76.1	69.7	92	19.2	0.52	0.57	0.46
Binxianbei S1	67.5	27.2	1800	145	115	0.0	3539	247,187	28.9	44.7	75	14.1	0.28	0.54	0.38
Yangling S1	50.3	16.3	3219	251	204	25.6	3746	191,348	5.6	22.8	143	19.4	0.06	0.18	0.68
Hongde S2-1	50.1	25.6	2649	127	69	41.1	8482	191,016	46.9	78.1	80	17.4	1.07	0.48	0.35
Baimapu S2-1	65.6	21.6	1580	107	67	15.4	2065	231,821	32.4	43.0	52	13.3	0.33	0.50	0.27
Binxianbei S2-1	55.0	18.2	2083	164	62	68.4	2428	192,757	12.6	48.6	83	15.2	0.09	0.35	0.59
Yangling S2-1	60.3	21.3	2203	159	88	37.9	2587	211,879	28.9	66.0	74	14.5	0.39	0.46	0.56

Chemical composition of the acetic acid-leachable fraction is expressed relative to the total mass of the original samples.

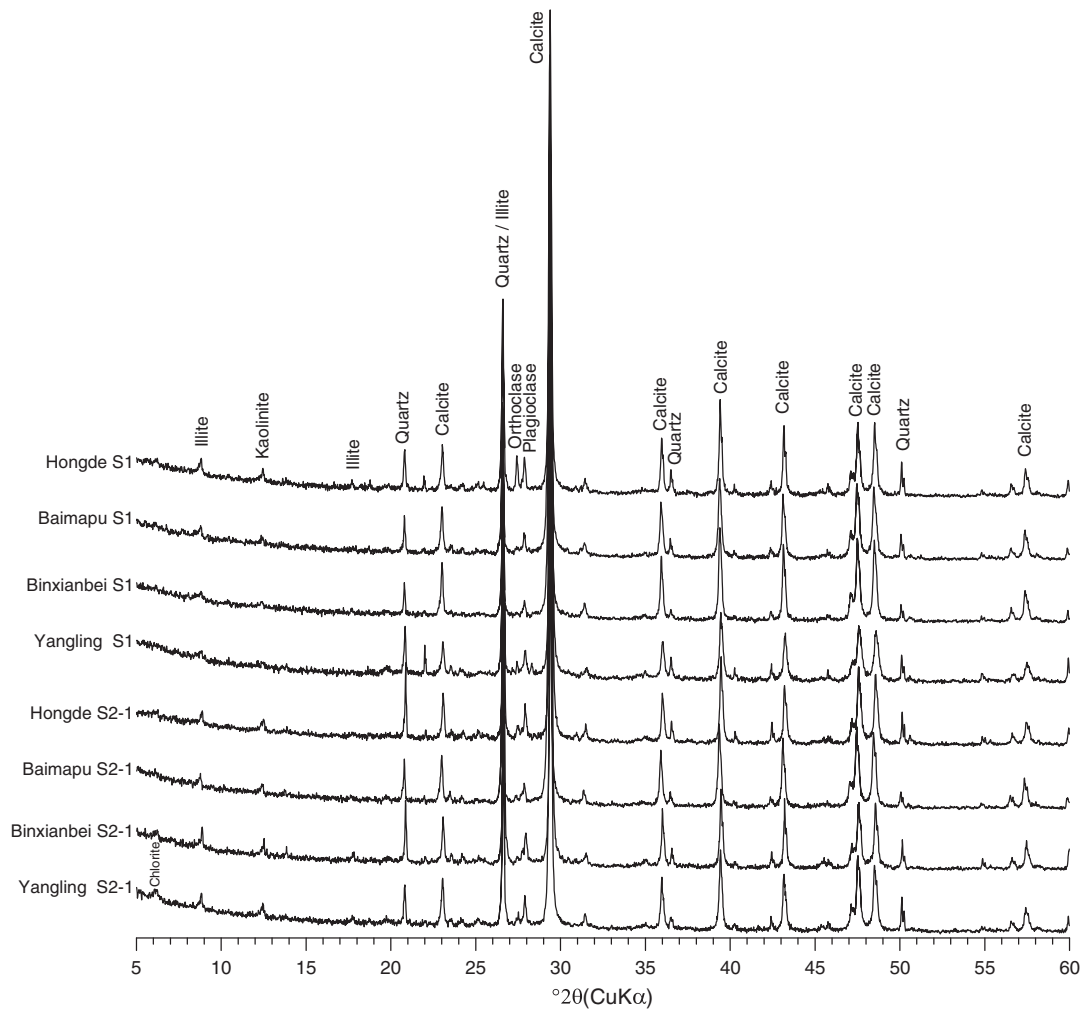


Fig. 3. XRD patterns for carbonate nodules of soil units S1 and S2-1 from the Hongde–Yangling loess transect.

from 25–40 ppm to 15–22 ppm, while the concentrations of Al and Si increase from 90–130 ppm to 150–250 ppm and from 40–70 ppm to 80–210 ppm, respectively. The U concentration also shows a southward increase (from 0.3–0.35 ppm to 0.5–0.7 ppm). Ca, K, and Mg, the most abundant elements in the acetic acid-leachable fraction, do not show any regular spatial pattern, and neither do Sr and Ba.

5. Sources of elements

Chemical composition of soil solution is essentially controlled by the mineralogical composition of soil and climate conditions. Chinese loess is a highly homogeneous mixture of atmospheric dust derived from a huge area with various bed rocks (Liu, 1985), and thus shows a remarkable degree of chemical homogeneity (Ding et al., 2001a; Jahn et al., 2001; Yang et al., 2006). Thus the soil solution composition in Chinese loess essentially reflects the rate and stage of soil weathering, which are ultimately controlled by climate.

As mentioned earlier, soil carbonate is a product of soil solution. Thus, to some extent, the pedogenic carbonate is an elemental sink while its overlying soil unit is an elemental source. For carbonate nodules, however, they are composed of authigenic calcite and its surrounding silicate minerals. As shown by the XRD results (Fig. 3), there are significant content of quartz, feldspar, and clay minerals in the carbonate nodules. Therefore, sources of the acetic acid-leachable elements need to be fully evaluated prior to any paleoclimatic interpretations.

Theoretically, most of the adsorbed cations were removed by NH_4 -acetate in the pretreatment process, thus the trace elements in the acid leachate mainly come from two sources: ions incorporated into the calcite structure (e.g., Mg^{2+} , Sr^{2+} , and Ba^{2+} ions substituting for Ca^{2+}) and non- CaCO_3 phases (e.g., salts and silicate minerals). If an element is incorporated into the calcite of carbonate nodules, there should be a positive correlation between the concentration of the incorporated element and the carbonate content. To further investigate the elemental sources, plots of the elemental abundance versus carbonate content were constructed (Fig. 5). In the carbonate nodules, the Ca concentration shows an excellent positive correlation with carbonate content (Fig. 5), confirming a predominant contribution of CaCO_3 phase to the Ca ions. Conversely, the Mg concentration varies inversely with carbonate content, indicating that Mg mainly comes from non- CaCO_3 phases, presumably from the trapped clay minerals. The U, Sr, and Ba concentrations show a slight negative correlation with carbonate content (Fig. 5), also implying a considerable contribution of clays to these elements.

The concentrations of K, Na, Al, and Si show no significant correlation with carbonate content (Fig. 5), indicating that these elements were leached from sources independent of carbonate dilution effect. In the soil environment, Na^+ is highly water-soluble and has a low affinity for adsorption to clays (Brady and Weil, 2000; Kurtz and Melsted, 1973). In Chinese loess, Na^+ , derived mainly from dissolution of soluble salts (Duvall et al., 2008; Guo et al., 1991), is transported in downward

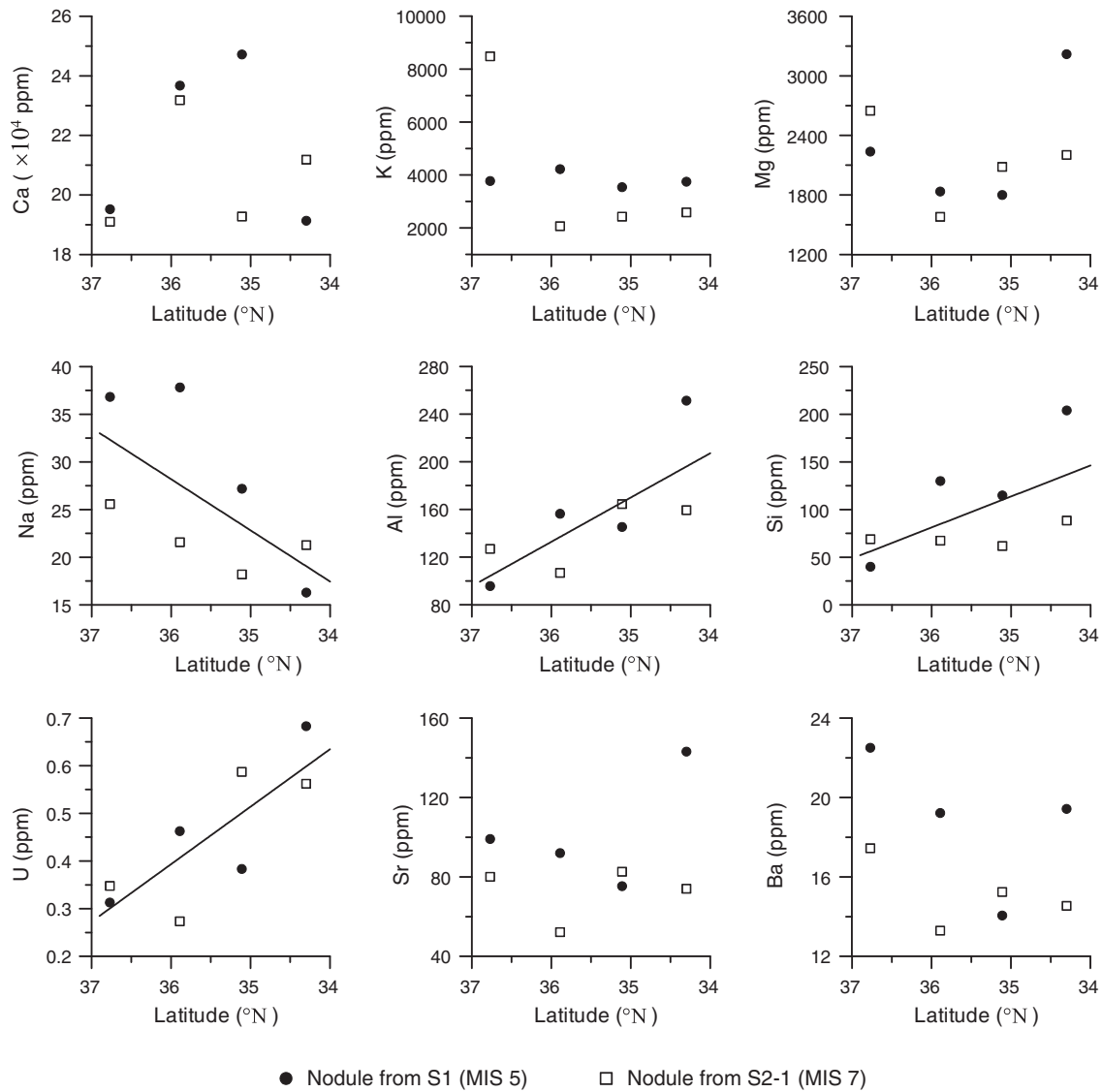


Fig. 4. Plots of acetic acid-leachable elemental concentration versus latitude for the carbonate nodules from soil units S1 and S2-1. The solid lines highlight the trends of elemental abundance changes along the north–south loess transect.

percolating soil water and may eventually reprecipitate as Na salts together with pedogenic carbonate. Therefore, the Na^+ in the acid leachate mainly comes from highly soluble salts, which may be trapped by calcite particles.

Potassium may be derived mainly from clay minerals, especially from illite, as indicated by the XRD patterns (Fig. 3). As the organic matter content is very low in Chinese loess (generally <0.5%) (Sun and Liu, 2000), it should be much lower in carbonate nodules than in loess deposits due to the dilution effect of carbonate. So the contribution of K from the organic matter should be minor. Altogether, our interpretations of sources of K, Mg, and Na are consistent with the findings of McNeal et al. (1985).

Aluminum and silicon are immobile, as they are bonded to the silicate framework. Although feldspar and clay minerals can release small amounts of Al and Si by reacting with acetic acid, this reaction generally requires long time, high temperature and/or concentrated acetic acid (Carroll and Starkey, 1971; Hamer et al., 2003; Huang and Kiang, 1972; Simon and Anderson, 1990; Stoessell and Pittman, 1990). Therefore, the Al and Si most likely come from amorphous phases of pedogenic origin (Baba and Okazaki, 2000; Cornelis et al., 2011; McKeague and Cline, 1963; Warren and Dudas, 1985).

6. Na/Al and Na/Si ratios as proxies for aridity

For most soils and soil materials, the order of relative affinities of major cations is $\text{Al}^{3+} > \text{Ca}^{2+} > \text{Mg}^{2+} > \text{K}^+ > \text{Na}^+$ (Brady and Weil, 2000; Kurtz and Melsted, 1973). Consequently, Na^+ tends to move farther and more readily in leaching and drainage waters. In soils, high content of soluble Na salts reflects an arid environment (Guo et al., 1991; Macdonald et al., 1999; Rengasamy and Olsson, 1991). Given the high water solubility of Na salts, the pattern of southward-decreasing Na content in the carbonate nodules (Fig. 4) indicates stronger leaching conditions in the south than in the north, i.e. a trend of increasing monsoon rainfall southward.

For the L1 loess unit at Mubo and Binxianbei, the water-soluble Na contents fall in the range 20–350 ppm and 20–160 ppm, respectively (unpublished data). Obviously, the Na contents in the carbonate nodules (15–40 ppm; Table 1 and Fig. 4) are comparable to or slightly lower than those in the loess deposits, which may result from a partial loss of Na during the NH_4 -acetate pretreatment. Therefore, the measured Na concentrations in the nodules (Table 1) are underestimated and should be regarded as lower limits. Despite these, the spatial pattern of Na content (Fig. 4) still indicates an unambiguous southward increase in monsoon

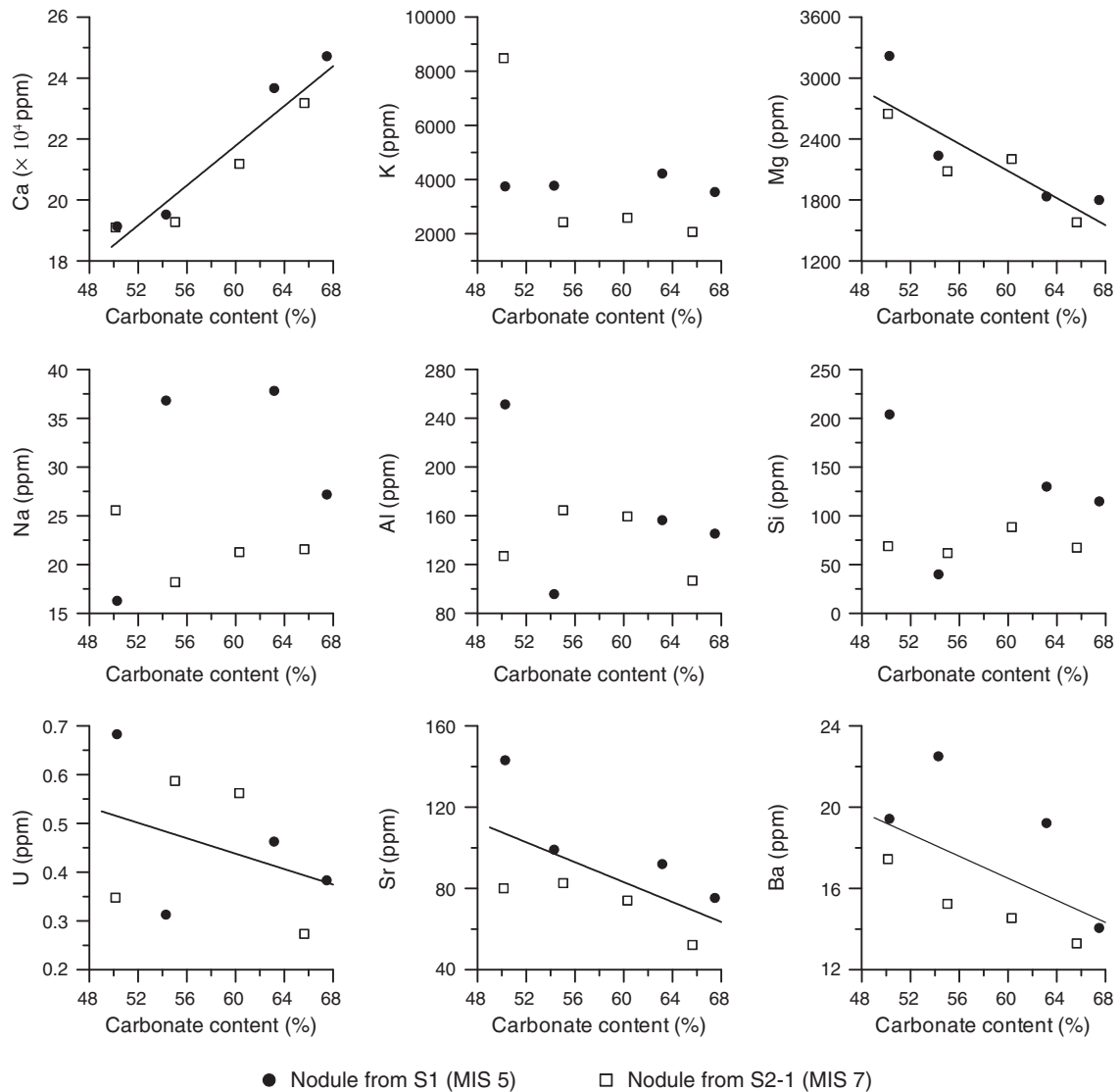


Fig. 5. Plots of acetic acid-leachable elemental concentration versus carbonate content for the carbonate nodules from soil units S1 and S2-1. The solid lines approximate the relationship between elemental abundance and carbonate content for the nodules.

precipitation across the Loess Plateau. Previous studies have shown that the precipitation of pedogenic carbonate results from dewatering of soil by evapotranspiration (Quade et al., 1989) and/or decrease in soil $p\text{CO}_2$ (Breecker et al., 2009). The significant soluble Na salts in the carbonate nodules indicate that soil dewatering is an important mechanism for the formation of carbonate nodules in Chinese loess, at least in the case of the northern Loess Plateau.

In Chinese loess, U is released into soil water as UO_2^{2+} during pedogenesis by weathering of accessory minerals (e.g., monazite and apatite) and carbonates (Gallet et al., 1996). When the downward soluble materials precipitate due to soil dewatering, U may be adsorbed onto and/or incorporated into clay minerals and amorphous ferric oxyhydroxide (e.g., Barnett et al., 2000; Morrison et al., 1995; Pogge von Strandmann et al., 2011; Porcelli et al., 2009). Therefore, high U content in carbonate nodules indicates conditions of relatively strong soil leaching. Thus the pattern of southward-increasing U in the nodules (Fig. 4) reflects a stronger summer monsoon in the south than in the north. The dissolved amorphous Al and Si increase from north to south (Fig. 4), also indicating enhanced soil leaching in the southern Loess Plateau. The opposite spatial pattern of Na to that of Al and Si (Fig. 4) leads to a consistent southward decrease in Na/Al and Na/Si values (Fig. 6), which can be

used as sensitive proxies for aridity, i.e. the lower these ratios the greater the summer monsoon precipitation.

7. Conclusions

Pedogenic carbonate nodules from Chinese loess have carbonate contents ranging from 50% to 68%. They are mainly composed of calcite, together with some silicate minerals such as quartz, plagioclase, orthoclase, illite, and kaolinite. In the acetic acid-leachable fraction of the carbonate nodules, Ca is the most abundant element, followed by K, Mg, Al, Si, Sr, Mn, Fe, P, Na, Ba, Pb, Th, and U. Based on the mineralogical data and relationship between carbonate and the leachable element content, we found that K, Mg, Sr, Ba, and U mainly come from clay minerals, Na from highly soluble salts trapped by calcite particles, and Al and Si from amorphous phases of pedogenic origin. The Na content shows a southward-decreasing pattern, while the Al, Si, and U concentrations display a southward-increasing pattern. These spatial patterns all suggest a southward decrease in aridity across the Chinese Loess Plateau for the last and penultimate interglacial periods, consistent with the pattern of a southerly increase in pedogenic development for the two interglacial soils, and with the pattern of the present north–south

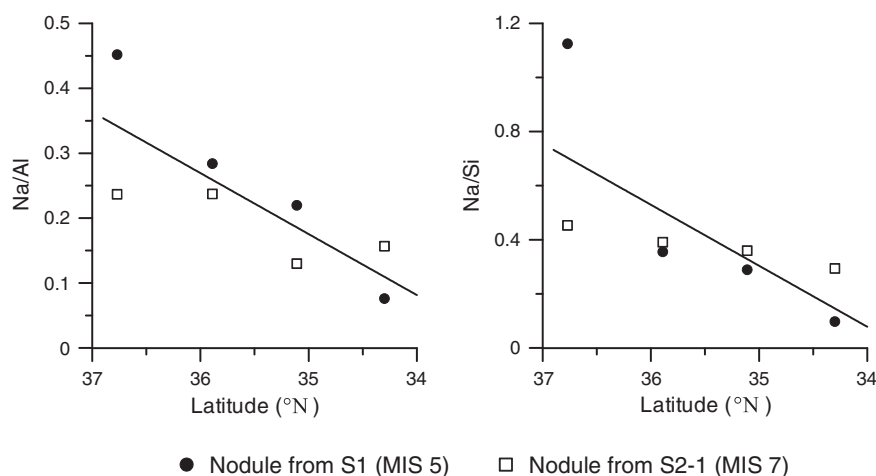


Fig. 6. Plots of acetic acid-leachable Na/Al (molar ratio) and Na/Si (molar ratio) versus latitude for the carbonate nodules from soil units S1 and S2-1. The solid lines highlight the spatial trends of Na/Al and Na/Si.

rainfall gradient. Therefore, Na/Al and Na/Si ratios in the acetic acid-leachable fraction of the carbonate nodules can serve as robust proxies for aridity, i.e. the lower these ratios the higher the summer monsoon rainfall. In addition, the significant content of soluble Na salts in the carbonate nodules highlights soil dewatering as an important mechanism for the formation of the nodules, at least in the case of the northern Loess Plateau.

Acknowledgments

This study is supported by the Strategic Priority Research Program of the Chinese Academy of Sciences (Grant Nos. XDA05120204 and XDB03020503), the National Basic Research Program of China (973 Program) (Grant No. 2010CB950204), and the National Natural Science Foundation of China (Grant No. 40972228). We thank Jay Quade, Amanda C. Reynolds, Qian Zhou, Yangyang Li, and Xiaozong Ren for the assistance in the laboratory, Shangfa Xiong, Xu Wang, and Shengshan Hou for the assistance in the field, and Jingtai Han, Chunxia Zhang, Li Yang, He Li, and Yueheng Yang for valuable discussions. We also thank two anonymous reviewers for their constructive comments that helped us to substantially improve this manuscript.

References

An, Z.S., Kukla, G., Porter, S.C., Xiao, J.L., 1991a. Late quaternary dust flow on the Chinese Loess Plateau. *Catena* 18, 125–132.

An, Z., Kukla, G.J., Porter, S.C., Xiao, J., 1991b. Magnetic susceptibility evidence of monsoon variation on the Loess Plateau of central China during the last 130,000 years. *Quaternary Research* 36, 29–36.

Baba, M., Okazaki, M., 2000. Changes in aluminum pools of aridisols due to soil acidification. *Soil Science and Plant Nutrition* 46, 797–805.

Barnett, M.O., Jardine, P.M., Brooks, S.C., Selim, H.M., 2000. Adsorption and transport of uranium(VI) in subsurface media. *Soil Science Society of America Journal* 64, 908–917.

Brady, N.C., Weil, R.R., 2000. *Elements of the Nature and Properties of Soils*. Prentice Hall, Upper Saddle River, New Jersey.

Breecker, D.O., Sharp, Z.D., McFadden, L.D., 2009. Seasonal bias in the formation and stable isotopic composition of pedogenic carbonate in modern soils from central New Mexico, USA. *Geological Society of America Bulletin* 121, 630–640.

Carroll, D., Starkey, H.C., 1971. Reactivity of clay minerals with acids and alkalis. *Clays and Clay Minerals* 19, 321–333.

Chen, J., Ji, J.F., Qiu, G., Lu, H.Y., 1998. Geochemical studies on the intensity of chemical weathering in Luochuan loess–paleosol sequence, China. *Science in China (Series D)* 41, 235–241.

Chen, J., An, Z.S., Head, J., 1999. Variation of Rb/Sr ratios in the loess–paleosol sequences of central China during the last 130,000 years and their implications for monsoon paleoclimatology. *Quaternary Research* 51, 215–219.

Cornelis, J.-T., Delvaux, B., Georg, R.B., Lucas, Y., Ranger, J., Opfergelt, S., 2011. Tracing the origin of dissolved silicon transferred from various soil–plant systems towards rivers: a review. *Biogeosciences* 8, 89–112.

Derbyshire, E., Kemp, R., Meng, X., 1995. Variations in loess and palaeosol properties as indicators of palaeoclimatic gradients across the Loess Plateau of North China. *Quaternary Science Reviews* 14, 681–697.

Ding, Z.L., Yang, S.L., 2000. C₃/C₄ vegetation evolution over the last 7.0 Myr in the Chinese Loess Plateau: evidence from pedogenic carbonate δ¹³C. *Palaeogeography Palaeoclimatology Palaeoecology* 160, 291–299.

Ding, Z.L., Rutter, N., Liu, T.S., 1993. Pedostratigraphy of Chinese loess deposits and climatic cycles in the last 2.5 Myr. *Catena* 20, 73–91.

Ding, Z.L., Ren, J.Z., Yang, S.L., Liu, T.S., 1999. Climate instability during the penultimate glaciation: evidence from two high-resolution loess records, China. *Journal of Geophysical Research* 104, 20123–20132.

Ding, Z.L., Sun, J.M., Yang, S.L., Liu, T.S., 2001a. Geochemistry of the Pliocene red clay formation in the Chinese Loess Plateau and implications for its origin, source provenance and paleoclimate change. *Geochimica et Cosmochimica Acta* 65, 901–913.

Ding, Z.L., Yang, S.L., Sun, J.M., Liu, T.S., 2001b. Iron geochemistry of loess and red clay deposits in the Chinese Loess Plateau and implications for long-term Asian monsoon evolution in the last 7.0 Ma. *Earth and Planetary Science Letters* 185, 99–109.

Ding, Z.L., Derbyshire, E., Yang, S.L., Yu, Z.W., Xiong, S.F., Liu, T.S., 2002. Stacked 2.6-Ma grain size record from the Chinese loess based on five sections and correlation with the deep-sea δ¹⁸O record. *Paleoceanography* 17, 1033. <http://dx.doi.org/10.1029/2001PA000725>.

Duvall, R.M., Majestic, B.J., Shafer, M.M., Chuang, P.Y., Simoneit, B.R.T., Schauer, J.J., 2008. The water-soluble fraction of carbon, sulfur, and crustal elements in Asian aerosols and Asian soils. *Atmospheric Environment* 42, 5872–5884.

Eden, D.N., Wen, Q.Z., Hunt, J.L., Whitton, J.S., 1994. The mineralogical and geochemical trends across the Loess Plateau, North China. *Catena* 21, 73–90.

English, N.B., Quade, J., DeCelles, P.G., Garzzone, C.N., 2000. Geologic control of Sr and major element chemistry in Himalayan Rivers, Nepal. *Geochimica et Cosmochimica Acta* 64, 2549–2566.

Gallet, S., Jahn, B.M., Torii, M., 1996. Geochemical characterization of the Luochuan loess–paleosol sequence, China and paleoclimatic implications. *Chemical Geology* 133, 67–88.

Gu, Z.Y., Lal, D., Liu, T.S., Guo, Z.T., Southon, J., Caffee, M.W., 1997. Weathering histories of Chinese loess deposits based on uranium and thorium series nuclides and cosmogenic ¹⁰Be. *Geochimica et Cosmochimica Acta* 61, 5221–5231.

Gu, Z.Y., Ding, Z.L., Xiong, S.F., Liu, T.S., 1999. A seven million geochemical record from Chinese red-clay and loess–paleosol sequence: weathering and erosion in northwestern China. *Quaternary Sciences* 19, 357–365 (in Chinese with English abstract).

Guo, Z., Fedoroff, N., An, Z., 1991. Genetic types of the Holocene soil and the Pleistocene paleosols in the Xifeng loess section in central China. In: Liu, T. (Ed.), *Loess, Environment and Global Change*. Science Press, Beijing, pp. 93–111.

Guo, Z., Biscaye, P., Wei, L., Chen, X., Peng, S., Liu, T., 2000. Summer monsoon variations over the last 1.2 Ma from the weathering of loess–soil sequences in China. *Geophysical Research Letters* 27, 1751–1754.

Gyölesjö, S., Arnold, E., 2006. Clay mineralogy of a red clay–loess sequence from Lingtai, the Chinese Loess Plateau. *Global and Planetary Change* 51, 181–194.

Hamer, M., Graham, R.C., Amrhein, C., Bozhilov, K.N., 2003. Dissolution of ripidolite (Mg, Fe-chlorite) in organic and inorganic acid solutions. *Soil Science Society of America Journal* 67, 654–661.

Han, J., Keppens, E., Liu, T., Paepe, R., Jiang, W., 1997. Stable isotope composition of the carbonate concretion in loess and climate change. *Quaternary International* 37, 37–43.

Han, J., Fyfe, W.S., Longstaffe, F.J., 1998. Climatic implications of the S5 paleosol complex on the southernmost Chinese Loess Plateau. *Quaternary Research* 50, 21–33.

Huang, W.H., Kiang, W.C., 1972. Laboratory dissolution of plagioclase feldspars in water and organic acids at room temperature. *American Mineralogist* 57, 1849–1859.

Huang, C.Q., Zhao, W., Li, F.Y., Tan, W.F., Wang, M.K., 2012. Mineralogical and pedogenic evidence for palaeoenvironmental variations during the Holocene on the Loess Plateau, China. *Catena* 96, 49–56.

- Jahn, B.M., Gallet, S., Han, J.M., 2001. Geochemistry of the Xining, Xifeng and Jixian sections, Loess Plateau of China: eolian dust provenance and paleosol evolution during the last 140 ka. *Chemical Geology* 178, 71–94.
- Ji, J., Chen, J., Lu, H., 1999. Origin of illite in the loess from the Luochuan area, Loess Plateau, Central China. *Clay Minerals* 34, 525–532.
- Jiang, W.Y., Han, J.M., Liu, T.S., Yu, F.J., 1995. Stable isotope composition of inclusive water in the carbonate concretion in loess. *Scientia Geologica Sinica (Supplementary Issue (1))*, 73–79.
- Jiang, W.Y., Han, J.M., Liu, T.S., Chen, J.S., Wen, C.F., 1998. Stable isotopes of carbonate in Chinese loess as evidence of paleoenvironmental changes. In: Novak, M., Rosenbaum, J. (Eds.), *Challenges to Chemical Geology*. The Czech Geological Survey, Prague, pp. 175–186.
- Kukla, G., 1987. Loess stratigraphy in central China. *Quaternary Science Reviews* 6, 191–219.
- Kurtz, L.T., Melsted, S.W., 1973. Movement of chemicals in soils by water. *Soil Science* 115, 231–239.
- Lisiecki, L.E., Raymo, M.E., 2005. A Pliocene–Pleistocene stack of 57 globally distributed benthic $\delta^{18}\text{O}$ records. *Paleoceanography* 20, PA1003. <http://dx.doi.org/10.1029/2004PA001071>.
- Liu, T.S., 1985. *Loess and the Environment*. China Ocean Press, Beijing.
- Liu, T., Ding, Z., 1998. Chinese loess and the paleomonsoon. *Annual Review of Earth and Planetary Sciences* 26, 111–145.
- Liu, T.S., Guo, Z.T., Liu, J.Q., Han, J.M., Ding, Z.L., Gu, Z.Y., Wu, N.Q., 1995. Variations of eastern Asian monsoon over the last 140,000 years. *Bulletin de la Societe Geologique de France* 166, 221–229.
- Lu, Y.C., Wang, X.L., Wintle, A.G., 2007. A new OSL chronology for dust accumulation in the last 130,000 yr for the Chinese Loess Plateau. *Quaternary Research* 67, 152–160.
- Lyle, M., Heath, G.R., Robbins, J.M., 1984. Transport and release of transition elements during early diagenesis: sequential leaching of sediments from MANOP Sites M and H. Part I. pH 5 acetic acid leach. *Geochimica et Cosmochimica Acta* 48, 1705–1715.
- Macdonald, B.C.T., Melville, M.D., White, I., 1999. The distribution of soluble cations within chenopod-patterned ground, arid western New South Wales, Australia. *Catena* 37, 89–105.
- McKeague, J.A., Cline, M.G., 1963. Silica in soil solutions II The adsorption of monosilicic acid by soil and by other substances. *Canadian Journal of Soil Science* 43, 83–96.
- McNeal, J.M., Severson, R.C., Gough, L.P., 1985. The occurrence of extractable elements in soils from the northern Great Plains. *Soil Science Society of America Journal* 49, 873–881.
- Morrison, S.J., Spangler, R.R., Tripathi, V.S., 1995. Adsorption of uranium(VI) on amorphous ferric oxyhydroxide at high concentrations of dissolved carbon(IV) and sulfur(VI). *Journal of Contaminant Hydrology* 17, 333–346.
- Pogge von Strandmann, P.A.E., Burton, K.W., Porcelli, D., James, R.H., van Calsteren, P., Gislason, S.R., 2011. Transport and exchange of U-series nuclides between suspended material, dissolved load and colloids in rivers draining basaltic terrains. *Earth and Planetary Science Letters* 301, 125–136.
- Porcelli, D., Strekopytov, S., Shaw, S., Baskaran, M., Hilton, D., Kulongoski, J., 2009. Isotopic and experimental constraints on subsurface U transport and fate. *Research Abstracts 11 (EGU2009-8645, 6th EGU General Assembly)*.
- Quade, J., Cerling, T.E., Bowman, J.R., 1989. Systematic variations in the carbon and oxygen isotopic composition of pedogenic carbonate along elevation transects in the southern Great Basin, United States. *Geological Society of America Bulletin* 101, 464–475.
- Quade, J., Chivas, A.R., McCulloch, M.T., 1995. Strontium and carbon isotope tracers and the origins of soil carbonate in South Australia and Victoria. *Palaeogeography Palaeoclimatology Palaeoecology* 113, 103–117.
- Rengasamy, P., Olsson, K.A., 1991. Sodicity and soil structure. *Australian Journal of Soil Research* 29, 935–952.
- Rutter, N., Ding, Z., 1993. Paleoclimates and monsoon variations interpreted from micromorphogenic features of the Baoji paleosols, China. *Quaternary Science Reviews* 12, 853–862.
- Rutter, N.W., Ding, Z.L., Evans, M.E., Liu, T.S., 1991. Baoji-type pedostratigraphic section, Loess Plateau, north-central China. *Quaternary Science Reviews* 10, 1–22.
- Simon, D.E., Anderson, M.S., 1990. Stability of clay minerals in acid. Paper SPE 19422 presented at the SPE Formation Damage Control Symposium, Lafayette, Louisiana, February 22–23, 1990. Society of Petroleum Engineers Incorporated 201–212.
- Soil Conservation Service, 1972. *Soil Survey Laboratory Methods and Procedures for Collecting Soil Samples*. U.S. Department of Agriculture, Washington, D.C.
- Stoessell, R.K., Pittman, E.D., 1990. Secondary porosity revisited: the chemistry of feldspar dissolution by carboxylic acids and anions. *American Association of Petroleum Geologists Bulletin* 74, 1795–1805.
- Sun, J., Liu, T., 2000. Multiple origins and interpretations of the magnetic susceptibility signal in Chinese wind-blown sediments. *Earth and Planetary Science Letters* 180, 287–296.
- Van der Hoven, S.J., Quade, J., 2002. Tracing spatial and temporal variations in the sources of calcium in pedogenic carbonates in a semiarid environment. *Geoderma* 108, 259–276.
- Wang, Y., Zheng, S.H., 1989. Paleosol nodules as Pleistocene paleoclimatic indicators, Luochuan, P.R. China. *Palaeogeography Palaeoclimatology Palaeoecology* 76, 39–44.
- Warren, C.J., Dudas, M.J., 1985. Formation of secondary minerals in artificially weathered fly ash. *Journal of Environmental Quality* 14, 405–410.
- Xiong, S.F., Ding, Z.L., Jiang, W.Y., Yang, S.L., Liu, T.S., 2003. Initial intensification of East Asian winter monsoon at about 2.75 Ma as seen in the Chinese eolian loess–red clay deposit. *Geophysical Research Letters* 30, 1524. <http://dx.doi.org/10.1029/2003GL017059>.
- Xiong, S., Ding, Z., Zhu, Y., Zhou, R., Lu, H., 2010. A 6 Ma chemical weathering history, the grain size dependence of chemical weathering intensity, and its implications for provenance change of the Chinese loess–red clay deposit. *Quaternary Science Reviews* 29, 1911–1922.
- Yang, S.L., Ding, Z.L., 2003. Color reflectance of Chinese loess and its implications for climate gradient changes during the last two glacial–interglacial cycles. *Geophysical Research Letters* 30, 2058. <http://dx.doi.org/10.1029/2003GL018346>.
- Yang, S.L., Ding, Z.L., 2004. Comparison of particle size characteristics of the Tertiary ‘red clay’ and Pleistocene loess in the Chinese Loess Plateau: implications for origin and sources of the ‘red clay’. *Sedimentology* 51, 77–93.
- Yang, S., Ding, Z., 2008. Advance–retreat history of the East-Asian summer monsoon rainfall belt over northern China during the last two glacial–interglacial cycles. *Earth and Planetary Science Letters* 274, 499–510.
- Yang, S., Ding, Z., 2010. Drastic climatic shift at 2.8 Ma as recorded in eolian deposits of China and its implications for redefining the Pliocene–Pleistocene boundary. *Quaternary International* 219, 37–44.
- Yang, S., Ding, F., Ding, Z., 2006. Pleistocene chemical weathering history of Asian arid and semi-arid regions recorded in loess deposits of China and Tajikistan. *Geochimica et Cosmochimica Acta* 70, 1695–1709.
- Yang, S., Ding, Z., Wang, X., Tang, Z., Gu, Z., 2012. Negative $\delta^{18}\text{O}$ – $\delta^{13}\text{C}$ relationship of pedogenic carbonate from northern China indicates a strong response of C_3/C_4 biomass to the seasonality of Asian monsoon precipitation. *Palaeogeography Palaeoclimatology Palaeoecology* 317 (318), 32–40.